



New Gogny interaction suitable for astrophysical applications

C. Gonzalez-Boquera^{a,*}, M. Centelles^a, X. Viñas^a, L.M. Robledo^{b,c}

^a Departament de Física Quàntica i Astrofísica and Institut de Ciències del Cosmos (ICCUB), Facultat de Física, Universitat de Barcelona, Martí i Franquès 1, E-08028 Barcelona, Spain

^b Departamento de Física Teórica, Facultad de Física, Universidad Autónoma de Madrid, E-28049 Madrid, Spain

^c Center for Computational Simulation, Universidad Politécnica de Madrid, Campus de Montegancedo, Boadilla del Monte, 28660-Madrid, Spain

ARTICLE INFO

Article history:

Received 19 December 2017

Received in revised form 29 January 2018

Accepted 3 February 2018

Available online 6 February 2018

Editor: J.-P. Blaizot

ABSTRACT

The D1 family of parametrizations of the Gogny interaction commonly suffers from a rather soft neutron matter equation of state that leads to maximal masses of neutron stars well below the observational value of two solar masses. We propose a reparametrization scheme that preserves the good properties of the Gogny force but allows one to tune the density dependence of the symmetry energy, which, in turn, modifies the predictions for the maximum stellar mass. The scheme works well for D1M, and leads to a new parameter set, dubbed D1M*. In the neutron-star domain, D1M* predicts a maximal mass of two solar masses and global properties of the star in harmony with those obtained with the Sly4 Skyrme interaction. By means of a set of selected calculations in finite nuclei, we check that D1M* performs comparably well to D1M in several aspects of nuclear structure in nuclei.

© 2018 The Authors. Published by Elsevier B.V. This is an open access article under the CC BY license (<http://creativecommons.org/licenses/by/4.0/>). Funded by SCOAP³.

1. Introduction

Neutron stars (NSs) are among the densest objects in the Universe. From the surface to the center of a NS the density varies by about fifteen orders of magnitude, involving several physical scenarios [1,2]. The outermost part of the star, or outer crust, consists of ionized atomic nuclei embedded in a free electron gas. These nuclei arrange themselves in a solid lattice to minimize the Coulomb repulsion and are stabilized against β -decay by the electron gas [2,3]. In the deepest layers of the outer crust, nuclei become so neutron rich that neutrons start to drip. Hence, the structure of the inner crust consists of a Coulomb lattice of nuclear clusters permeated by free neutron and electron gases (see e.g. [4–6] and refs. therein). At the bottom of this region, the nuclear clusters may adopt non-spherical shapes (“nuclear pasta”) in order to minimize the Coulomb energy. The inner crust extends up to densities about one half of the saturation density of nuclear matter ($\simeq 1.3 \times 10^{14}$ g/cm³). In the interior region of a NS, or core, matter forms a homogeneous liquid composed of neutrons plus a certain fraction of protons, electrons and muons, and eventually other exotic particles, under β -equilibrium and charge neutrality [1,2]. This region accommodates most of the mass and size of the star, implying that global properties such as the maximum mass,

radius, or moment of inertia of the NS are determined to a large extent by the properties of the homogeneous core.

From a theoretical point of view, the essential ingredient to study NSs is the equation of state (EOS) of matter [7]. Although nowadays sophisticated ab initio calculations can be performed to describe the homogeneous matter in the core, effective nuclear interactions such as Skyrme forces or the relativistic mean field (RMF) theory, which successfully describe many properties of terrestrial nuclei, are in wide use for NS calculations due to their relative simplicity. For instance, Skyrme-HFB models [8] have reached a high degree of accuracy in predicting experimental masses and are at the same time well suited for astrophysical studies [9,10]. More occasionally, also Gogny forces have been applied in NS calculations [11–16]. Due to the complexity of modeling the inner crust, there are few EOSs that describe the whole NS from the crust to the core in a unified manner. Some examples are, among others [7], the EOS of Lattimer–Swesty [17], the SLy EOS of Douchin–Haensel [5], the EOSs of the BSk family developed by the Brussels group [9,10], which are based on Skyrme forces, the EOS by Shen et al. [18] obtained within the RMF theory, or the BCPM EOS based on Brueckner calculations [6].

In Skyrme forces the interaction is of zero range and the pairing force, which is needed to study open-shell nuclei, is not connected with the force used to describe the mean field. The Gogny interaction was proposed more than thirty years ago aimed to describe the mean field and the pairing field simultaneously with the same

* Corresponding author.

E-mail address: cgonzalezboquera@ub.edu (C. Gonzalez-Boquera).

finite-range effective force [19]. Large-scale HFB calculations based on the D1S Gogny parametrization [20] revealed some deficiencies in the description of nuclear masses compared to experimental data. To overcome these limitations, new Gogny parametrizations such as D1N [21] and D1M [22] have been proposed. At variance with D1S and D1N, which follow the D1 fitting protocol [19], the D1M force has been fitted by minimizing the difference to 2149 measured nuclear masses [23] and including quadrupole correlation energies. It is important to mention that in the calibration of D1N and D1M, the energy of neutron matter is required to qualitatively reproduce the microscopic calculations of Friedman and Pandharipande [24]. D1M reproduces the 2149 experimental masses with a rms deviation as low as 798 keV [22]. Unfortunately, the extrapolation to the domain of neutron stars with the Gogny parametrizations works less well. It has been found [13,15,16] that the most successful Gogny forces for describing finite nuclei, namely D1S, D1N and D1M, are unable to reach NS masses of about $2M_\odot$, as required by recent astrophysical observations [25,26]. Moreover, only few Gogny forces, including D1M but not D1N nor D1S, achieve a NS mass above the canonical $1.4M_\odot$ value [15,16]. Therefore, the aim of this work is to introduce a new Gogny force, which we call D1M*, that retaining a similar quality to D1M for finite nuclei, may be used to study NS physics at a level of the most successful Skyrme forces. We next analyze the neutron-star matter EOS and the predictions for NS masses and radii provided by different Gogny forces, and, specially, by D1M*. The fit of the new force D1M* is discussed afterwards, and its ability for describing infinite nuclear matter and finite nuclei is investigated.

2. Neutron-star matter described with Gogny interactions

The standard Gogny interaction of the D1 family consists of a finite-range part, which is modeled by two Gaussian terms including all the possible spin-isospin exchange terms, plus a zero-range density-dependent term. Adding the spin-orbit force, which is also of contact type, the Gogny interaction reads [19]:

$$V(\mathbf{r}_1, \mathbf{r}_2) = \sum_{i=1,2} (W_i + B_i P_\sigma - H_i P_\tau - M_i P_\sigma P_\tau) e^{-r^2/\mu_i^2} + t_3(1 + x_3 P^\sigma) \rho^\alpha(\mathbf{R}) \delta(\mathbf{r}) + iW_{LS}(\sigma_1 + \sigma_2)(\mathbf{k}' \times \delta(\mathbf{r})\mathbf{k}), \quad (1)$$

where \mathbf{r} and \mathbf{R} are the relative and the center of mass coordinates of the two nucleons, and $\mu_1 \simeq 0.5\text{--}0.7\text{ fm}$ and $\mu_2 \simeq 1.2\text{ fm}$ are the ranges of the two Gaussian form factors, which simulate the short- and long-range components of the force, respectively. In Eq. (1), $\mathbf{k} = (\vec{\nabla}_1 - \vec{\nabla}_2)/2i$ is the relative momentum between the two nucleons and \mathbf{k}' is its complex conjugate.

The symmetry energy is the basic quantity that rules the isovector part of the interaction. It is obtained as $E_{\text{sym}}(\rho) = \frac{1}{2} \partial^2 E_b(\rho, \delta) / \partial \delta^2|_{\delta=0}$ from the energy per particle $E_b(\rho, \delta)$ in asymmetric nuclear matter of density $\rho = \rho_n + \rho_p$ and isospin asymmetry $\delta = (\rho_n - \rho_p)/\rho$, where ρ_n and ρ_p are the neutron and proton densities. In the Gogny interaction, the symmetry energy becomes [16]:

$$E_{\text{sym}}(\rho) = \frac{\hbar^2}{6m} \left(\frac{3\pi^2}{2} \right)^{2/3} \rho^{2/3} - \frac{t_3}{8} \rho^{\alpha+1} (2x_3 + 1) - \frac{1}{6\sqrt{\pi}} \times \sum_{i=1,2} \left\{ \mu_i^3 k_F^3 \left(H_i + \frac{M_i}{2} \right) + \frac{(1 - e^{-\mu_i^2 k_F^2})}{\mu_i k_F} (W_i + 2B_i - 2H_i - 4M_i) + \mu_i k_F [H_i + 2M_i - e^{-\mu_i^2 k_F^2} (W_i + 2B_i - H_i - 2M_i)] \right\}, \quad (2)$$

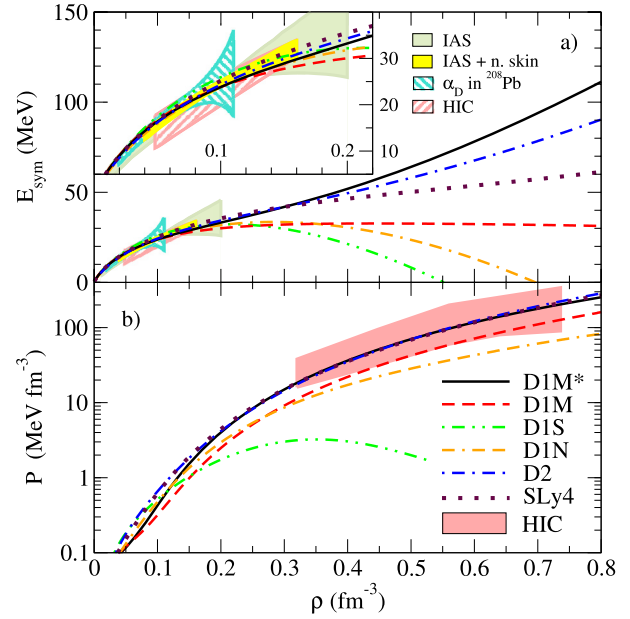


Fig. 1. a) Symmetry energy versus density from the D1S, D1N, D1M, D1M* and D2 Gogny forces and from the Sly4 Skyrme force. The inset is a magnified view of the low-density region. Also plotted are the constraints from isobaric analog states (IAS) and from IAS and neutron skins (IAS+n.skin) [28], from the electric dipole polarizability in lead (α_D in ^{208}Pb) [29] and from transport in heavy-ion collisions (HIC) [30]. b) Pressure in β -stable nuclear matter in logarithmic scale as a function of density for the same interactions of panel a). The shaded area depicts the region compatible with collective flow in HICs [31].

where $k_F = (3\pi^2 \rho/2)^{1/3}$ is the Fermi momentum. The slope parameter L , defined as $L = 3\rho_0 \partial E_{\text{sym}}(\rho) / \partial \rho|_{\rho=\rho_0}$ where ρ_0 is the saturation density, provides a good handle on the density dependence of the symmetry energy around saturation. The L value is known to be strongly correlated with the isospin properties, such as e.g. neutron densities and neutron skins, of nuclei [27].

The symmetry energy as a function of density is displayed in Fig. 1a for several Gogny forces and for the Sly4 Skyrme force, used in the NS Sly EOS of Douchin-Haensel [5]. At subsaturation densities the symmetry energy in the considered forces displays a similar behavior and takes a value of about 30 MeV at saturation. The subsaturation regime is also the finite nuclei regime, where the parameters of the nuclear forces are fitted to. Indeed, we observe in Fig. 1a that at subsaturation the present forces fall within or are very close to the region compatible with recent constraints on $E_{\text{sym}}(\rho)$ deduced from several nuclear observables [28–30]. Above saturation, in contrast, the behavior of the calculated symmetry energy shows a strong model dependence. The Gogny parametrizations usually extrapolate to high density with a too soft symmetry energy. For example, D1M shows a nearly flat behavior at suprasaturation, and the $E_{\text{sym}}(\rho)$ curves of D1S and D1N, after reaching a maximum at $\rho \sim 0.2\text{--}0.3\text{ fm}^{-3}$, bend down until they become negative at some density a few times the saturation one, which indicates the onset of an isospin instability. Although this happens at large densities for terrestrial phenomena, it is critical for neutron stars, where larger densities occur in the star's interior. The other Gogny forces in the figure, i.e., D2 [32] and the new D1M* force of this work, exhibit an increasing $E_{\text{sym}}(\rho)$ with growing density and do not present the isospin instability. D2 is a very recent Gogny interaction [32] devised by the Bruyères-le-Châtel group, where the usual zero-range density-dependent term of the D1 family is replaced by a finite-range term. As in the D1N and D1M cases, the fit of D2 requires the reproduction of the microscopic energy of neutron matter [24]. Concerning the results for

finite nuclei, D2 [32] describes the binding energies along isotopic chains without the drift of the energies with increasing neutron number observed in D1S [33]. However, as pointed out in [32], the global description of nuclear masses using the D2 force does not reach yet the quality obtained with D1M [22]. The D1M* force is a new Gogny parametrization of the type of Eq. (1), introduced here for the first time. It is devised to keep the quality of the description of finite nuclei at the level of D1M and to be able to predict NSs fulfilling the astrophysical observations of two solar masses. Details on the strategy followed to obtain D1M* and the parameters of this force are given later in Sec. 3.

The mass-radius (M - R) relation in neutron stars is dictated by the corresponding EOS, which is the essential ingredient to solve the Tolman–Oppenheimer–Volkov (TOV) equations [1]. The EOS (total pressure against density) of β -stable, globally charge-neutral NS matter [15,16] calculated with the given functionals is displayed in Fig. 1b. The new Gogny force D1M* and D2 predict a high-density EOS with a similar stiffness to the SLy4 EOS and they agree well with the region constrained by collective flow in energetic heavy-ion collisions (HIC) [31], shown as the shaded area in Fig. 1b.¹ The EOSs from the original D1M parametrization and from D1N are significantly softer. The D1S force yields a too soft EOS soon after saturation density, which implies it is not suitable for describing NSs.

To solve the TOV equations for a NS, knowledge of the EOS from the center to the surface of the star is needed. At present we do not have microscopic calculations of the EOS of the inner crust with Gogny forces. In this work, following previous literature [16,34–36], we interpolate the inner-crust EOS by a polytropic form $P = a + b\epsilon^{4/3}$ (ϵ is the mass-energy density), where the index $4/3$ assumes that the pressure at these densities is dominated by the relativistic degenerate electrons. We match this formula continuously to our Gogny EOSs of the homogeneous core and to the Haensel–Pichon EOS of the outer crust [5]. The core–crust transition density is selfconsistently computed for each Gogny force by the thermodynamical method [16]. We show in Fig. 2 the obtained NS mass–radius plots (results for D1S are not shown because D1S did not produce stable solutions of the TOV equations). We also plot as a benchmark the M - R curve calculated with the unified NS EOS proposed by Douchin and Haensel [5], which uses the Skyrme SLy4 force. It can be seen that standard Gogny forces, such as D1M and D1N, predict too low maximum stellar masses, with D1N being unable to generate masses above $1.4M_\odot$. We note that this common failure of conventional Gogny parametrizations [13,15,16] has been cured in the new D1M* force, which, as well as D2 and SLy4, is successful in reaching the masses of $2M_\odot$ observed in NSs [25,26]. This fact is directly related to the behavior of the EOS in β -stable matter. As can be seen by looking at Figs. 1b and 2, the stiffer the EOS at high density, the larger the maximum NS mass. Concerning the new D1M* force, it predicts a maximum NS mass of $2M_\odot$ with a radius of 10.2 km, and a canonical star of $1.4M_\odot$ with a radius of 11.6 km. These values for NS radii are in line with the recent astrophysical extractions of NS sizes from low-mass X-ray binaries and X-ray bursters that provide radii below 13 km for canonical mass stars (see the M - R constraints plotted in Fig. 2 [38, 39]).

We close this section by presenting some results for the moment of inertia of the NS and of its crust. Astronomical observations of binary pulsars can provide information about the moment of inertia of NSs, which in turn may impose constraints on the EOS [40]. In the slow-rotation regime, the NS moment of inertia can be

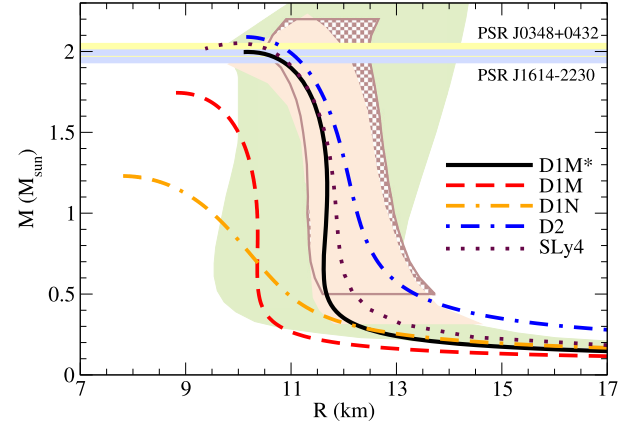


Fig. 2. Mass-radius relation in neutron stars from the D1N, D1M, D1M* and D2 Gogny forces and from the SLy4 Skyrme force (let us mention that for the shown results the speed of sound of these EOSs remains below the speed of light). The horizontal green bands of the figure depict the heaviest observed NS masses [25,26]. The vertical green band shows the allowed M - R region deduced from chiral nuclear interactions up to normal density plus astrophysically constrained high-density EOS extrapolations [37]. The brown dotted band is the zone constrained by the cooling tails of type-I X-ray bursts in three low-mass X-ray binaries and a Bayesian analysis [38], and the beige constraint at the front is from five quiescent low-mass X-ray binaries and five photospheric radius expansion X-ray bursters after a Bayesian analysis [39]. (For interpretation of the references to color in this figure legend, the reader is referred to the web version of this article.)

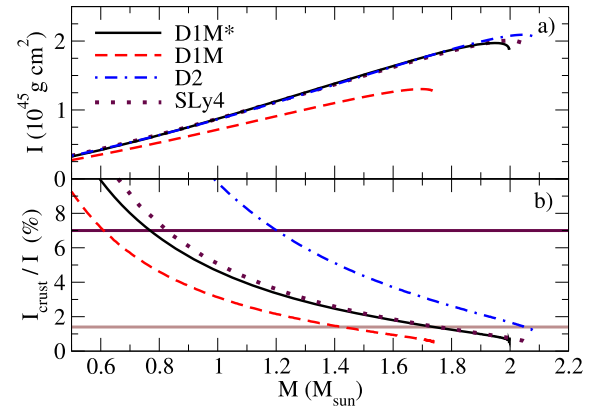


Fig. 3. a) Total moment of inertia of the neutron star, and b) crustal fraction of the moment of inertia, as functions of the total mass of the star. The horizontal lines in b) depict the bounds $I_{\text{crust}}/I > 1.4\%$ of [34] and $I_{\text{crust}}/I > 7\%$ of [43] from studying Vela pulsar glitches.

calculated by solving simultaneously the TOV equations and the differential equation for the moment of inertia in general relativity [41]. Our so-obtained results for the moment of inertia of the star are plotted in Fig. 3a. The predictions of D1M* and D2 are in close agreement with those from the SLy4 EOS. A precise measurement of I is expected within few years for pulsar A of the double system PSR J0737-3039 [42]. For the mass $1.34M_\odot$ of pulsar A, D1M*, D2 and SLy4 make a prediction of $I = 1.29 \times 10^{45} \text{ g cm}^2$.

Pulsar glitches may be indicative of the fraction of the moment of inertia stored in the crust. To explain the size of glitches observed in the Vela pulsar, initial studies suggested $I_{\text{crust}}/I > 1.4\%$ [34], while $I_{\text{crust}}/I > 7\%$ was obtained more recently by accounting for entrained neutrons in the crust [43] (also see Refs. [44–48] for recent studies of the constraints from pulsar glitches). The bounds of [34] and [43] are shown as horizontal lines in Fig. 3b. For either bound, the results for I_{crust}/I from D1M* suggest possible masses of the glitching source in between D2 and D1M. The predictions

¹ Though the constraint of [31] was proposed for neutron matter, at these densities the pressures of β -stable matter and neutron matter are very similar.

from D1M* are again found to be in consonance with those from the Sly4 EOS.

3. The fit of the D1M* interaction and further results

To determine the new Gogny interaction D1M*, we have modified the values of the parameters that control the stiffness of the symmetry energy while retaining as much as possible the quality of D1M for the binding energies and charge radii of nuclei. The basic concept is similar to previous literature where families of Skyrme and RMF parametrizations were generated starting from accurate models, as for example the SAMi-J [49], KDE0-J [50] or FSU-TAMU [51,52] families. In our case, we readjust the eight parameters W_i , B_i , H_i , M_i ($i = 1, 2$) of the finite-range part of the Gogny interaction (1), while the other parameters of Eq. (1) are kept fixed to the values of D1M. The open parameters are constrained by requiring the same saturation density, energy per particle, compressibility and effective mass in symmetric nuclear matter as in the original D1M force, and, in order to have a correct description of asymmetric nuclei, the same value of $E_{\text{sym}}(0.1)$, i.e., the symmetry energy at density 0.1 fm^{-3} . The last condition is based on the fact that the binding energies of finite nuclei constrain the symmetry energy at an average density of nuclei of about 0.1 fm^{-3} more tightly than at the saturation density ρ_0 [53, 54]. To preserve the pairing properties in the $S = 0$, $T = 1$ channel, we demand in the new force the same value of D1M for the two combinations of parameters $W_i - B_i - H_i + M_i$ ($i = 1, 2$). Thus, we are able to obtain seven of the eight free parameters of D1M* as a function of a single parameter, which we chose to be B_1 . This parameter is used to modify the slope L of the symmetry energy at saturation and, therefore, the behavior of the neutron matter EOS above saturation, which in turn determines the maximum mass of neutron stars. In this way the parameters of the finite-range part of the new interaction D1M* are completely determined. Finally, we perform a small readjustment of the zero-range strength t_3 to optimize the results for nuclear masses (see Sec. 3.1), which induces a slight change in the values of the saturation properties of uniform matter.

The parameters of the new force D1M* are collected in Table 1 and several nuclear matter properties in Table 2. Though the change in the W_i , B_i , H_i , M_i values is relatively large with respect to the D1M values [22], the saturation properties of symmetric nuclear matter and the symmetry energy at 0.1 fm^{-3} are basically the same as in D1M (see Table 2). The mainly modified property is the density dependence of the symmetry energy, with a change in the slope from $L = 24.83 \text{ MeV}$ to $L = 43.18 \text{ MeV}$, in order to provide a stiffer neutron matter EOS and limiting NS masses of $2M_\odot$. The different L value, as we fixed $E_{\text{sym}}(0.1)$, implies that the symmetry energy $E_{\text{sym}}(\rho_0)$ at saturation differs in D1M* from D1M. Table 2 also reports the nuclear matter properties of the other forces. It is particularly noticeable that L in D2 (44.85 MeV) is fairly larger than the values predicted by the D1 family and close to L obtained in D1M*.

A few recent bounds on $E_{\text{sym}}(\rho_0)$ and L proposed from analyzing different laboratory data and astrophysical observations [55–57] and from ab initio nuclear calculations using chiral interactions [58,59] are represented in Fig. 4. The prediction of D1M* is seen to overlap with the various constraints. We note this was not incorporated in the fit of D1M*. It follows as a consequence of having tuned the density dependence of the symmetry energy of the interaction to be able to reproduce heavy NS masses simultaneously with the properties of nuclear matter and nuclei. D2 and Sly4 also show good agreement with the constraints of Fig. 4. We observe that the three interactions have an $E_{\text{sym}}(\rho_0)$

Table 1

Parameters of the new D1M* Gogny interaction. W_i , B_i , H_i , M_i are in MeV, μ_i in fm, t_3 in MeV fm^4 , W_{LS} in MeV fm^5 , and x_3 and α are unitless.

D1M*	W_i	B_i	H_i	M_i	μ_i
$i = 1$	-17242.0144	19604.4056	-20699.9856	16408.3344	0.50
$i = 2$	675.3860	-982.8150	905.6650	-878.0060	1.00
<hr/>					
	t_3	x_3	α	W_{LS}	
	1561.22	1	1/3	115.36	

Table 2

Nuclear matter properties predicted by the D1M*, D1M, D1N, D1S and D2 Gogny interactions and the Sly4 Skyrme force.

	ρ_0 (fm^{-3})	E_0 (MeV)	K (MeV)	m^*/m	$E_{\text{sym}}(\rho_0)$ (MeV)	$E_{\text{sym}}(0.1)$ (MeV)	L (MeV)
D1M*	0.1650	-16.06	225.4	0.746	30.25	23.82	43.18
D1M	0.1647	-16.02	225.0	0.746	28.55	23.80	24.83
D1N	0.1612	-15.96	225.7	0.697	29.60	23.80	33.58
D1S	0.1633	-16.01	202.9	0.747	31.13	25.93	22.43
D2	0.1628	-16.00	209.3	0.738	31.13	24.32	44.85
Sly4	0.1596	-15.98	229.9	0.695	32.00	25.15	45.96

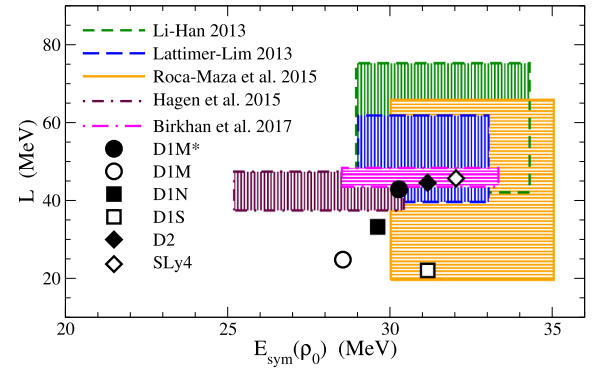


Fig. 4. Slope L and value $E_{\text{sym}}(\rho_0)$ of the symmetry energy at saturation density for the discussed interactions. The hatched regions are the experimental and theoretical constraints derived in [55–59].

value of 30–32 MeV and an L value of about 45 MeV. A similar feature was recently found in the frame of RMF models if the radii of canonical NSs are to be no larger than $\sim 13 \text{ km}$ [60,61]. It seems to us a remarkable fact the convergence of mean field models of different nature (Gogny, Skyrme, and RMF) to specific values $E_{\text{sym}}(\rho_0) \sim 30\text{--}32 \text{ MeV}$ and $L \sim 45 \text{ MeV}$ for the nuclear symmetry energy when the models successfully describe the properties of nuclear matter and finite nuclei and heavy neutron stars with compact stellar radii.

3.1. Finite nuclei

One of the goals of the present Gogny D1M* force is to preserve the good performance of D1M in describing nuclear structure features of finite nuclei. We have checked that the basic bulk properties of D1M*, such as binding energies or charge radii of even-even nuclei, remain globally unaltered as compared to D1M. The finite nuclei calculations have been carried out with the HFBaxial code [62] using an approximate second-order gradient method to solve the HFB equations [63] in a harmonic oscillator (HO) basis. The code preserves axial symmetry but is allowed to break reflection symmetry. It has already been used in large-scale calculations of nuclear properties with the D1M force, as e.g. in Ref. [64]. We carried out HFB calculations for 620 even-even nuclei of the 2012 AME [23] using the HFBaxial code. First, the potential energy surface (PES) as a function of the quadrupole moment Q_{20}

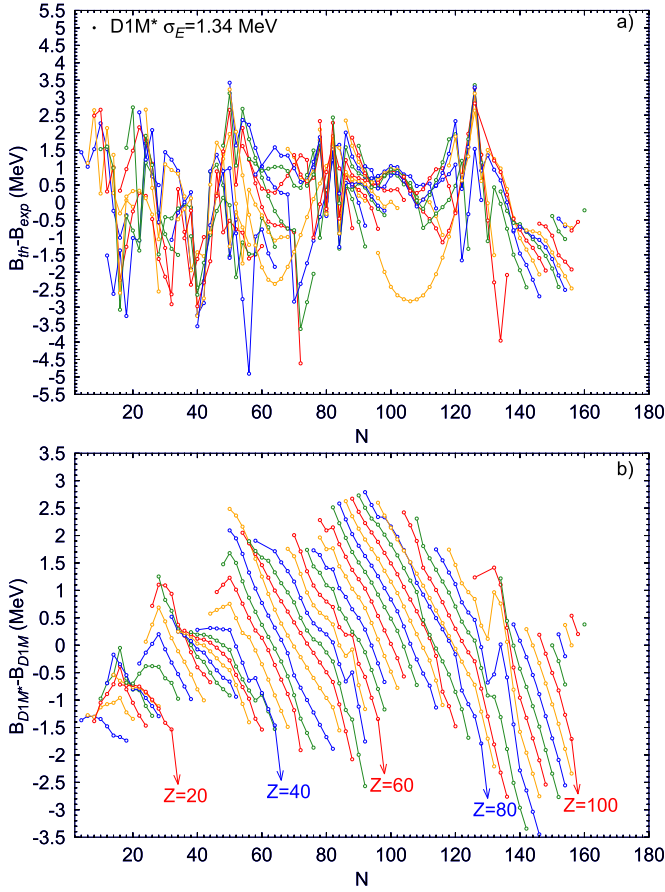


Fig. 5. a) Binding energy differences in 620 even-even nuclei between computed and experimental values [23] for the new D1M* force, as a function of neutron number N . b) Binding energy differences between the theoretical predictions of D1M* and D1M for 818 even-even nuclei.

is computed to select the lowest-energy minimum, which is subsequently used to start an unconstrained calculation to obtain the true HFB ground state. The binding energy is obtained by subtracting to the HFB energy the rotational energy correction, as given in Ref. [65]. The ground-state calculation is repeated with an enlarged basis containing two more HO major shells and an extrapolation scheme to an infinite HO basis is used to obtain the final binding energy [66,67]. In our framework, the zero-point energy (ZPE) of quadrupole motion used in the original fitting of D1M [22] is not taken into account because it requires considering β - γ PES and solving the five-dimensional collective Hamiltonian for all the nuclei. This is still an enormous task and we follow a different strategy where the quadrupole ZPE is replaced by a constant binding energy shift. This is somehow justified as in our experience the ZPE shows a weak mass dependence (see [68] for an example with the octupole degree of freedom). The energy shift is fixed by minimizing the global rms deviation, σ_E , for the known binding energies of 620 even-even nuclei [23]. With a shift of 2.7 MeV we obtain for D1M a σ_E of 1.36 MeV, which is larger than the 798 keV reported for D1M in [22] including also odd-even and odd-odd nuclei. The result is still satisfying and gives us confidence on the procedure followed. Using the same approach for D1M* we obtain a σ_E of 1.34 MeV (with a shift of 1.1 MeV), which compares favorably with our σ_E of 1.36 MeV for D1M.

The differences $\Delta B = B_{\text{th}} - B_{\text{exp}}$ between the binding energies of D1M* and the experimental values for 620 even-even nuclei belonging to different isotopic chains are displayed in Fig. 5a against the neutron number N . The ΔB values are scattered around zero

Table 3

Partial rms deviation (in MeV) from the experimental binding energies [23] in even-even nuclei, computed in the given mass-number intervals.

	$A \leq 80$	$80 < A \leq 160$	$A > 160$
D1M*	1.55	1.31	1.26
D1M	1.82	1.12	1.29

and show no drift with increasing N . The agreement between theory and experiment is specially good for medium-mass and heavy nuclei away from magic numbers and deteriorates for light nuclei, as may be seen from the partial σ_E deviations given in Table 3. From the partial σ_E values of Table 3, we also conclude that the closeness in the total σ_E of D1M and D1M* involves subtle cancellations that take place all over the nuclear chart. We plot the differences in binding energy predictions between D1M* and D1M in Fig. 5b against N for 818 even-even nuclei. A clear shift is observed as N increases within an isotopic chain. It is a direct consequence of the different density dependence of the symmetry energy in the two interactions. A similar behavior can be observed in a recent comparison [69] between D2 and D1S. It is also interesting to note that the results for neutron radii show a similar isotopic drift as the binding energies. Namely, the difference $r_{\text{D1M}^*} - r_{\text{D1M}}$ (where r is the rms radius computed from the HFB wave function) increases linearly with N for the neutron radii, whereas it remains essentially constant with N for the proton radii. This is again a consequence of the larger slope L of the symmetry energy in D1M* [54,70]. All these effects, as well as quadrupole, octupole and fission deformation properties of the new Gogny D1M* force will be analyzed in detail in forthcoming work. There are already indications of a good performance of D1M* in describing the basic parameters of fission.

4. Summary and conclusions

The existence of neutron stars with large masses of $2M_\odot$ [25, 26] has been exploited in recent years to select equations of state satisfying astrophysical evidence. The most successful forces of the D1 family of the finite-range Gogny interaction, which plays an important role in nuclear physics, have soft symmetry energies and fail to produce heavy enough stellar masses. We propose a way to reparametrize a Gogny force where, while preserving the description of nuclei, the slope of the symmetry energy can be modified as to make the EOS of β -stable matter stiffer to obtain NS masses of $2M_\odot$. The D1M force [22] is susceptible to being used in this procedure, but not D1S and D1N that are too far from the $2M_\odot$ target. We find that the new set of parameters, denoted as D1M*, is reconciled with the prediction of $2M_\odot$ stars and performs at the same level as D1M in all aspects of finite nuclei analyzed in this work. Stellar properties from D1M*, such as the M-R relation and the moment of inertia, are in good agreement with the results from the Douchin-Haensel SLy EOS [5]. Although much more work is required to assess the performance of D1M*, as e.g. in fission studies, we conclude that it represents a promising alternative in the description of nuclei and at the same time has the right properties to study exotic astrophysics scenarios such as NSs. We also have shown that the recent D2 Gogny model [32] fulfills the astrophysical requirement of $2M_\odot$ stars. However, when it comes to the applications in finite nuclei, D1M* is much less demanding than D2 in terms of computational resources [32]. For the time being, D1M* is more advantageous for the large-scale calculations required by applications as, for instance, in nuclear astrophysics (binding energies, fission barriers, etc.).

Acknowledgements

The work of LMR was supported by Spanish Ministry of Economy and Competitiveness (MINECO) Grants No. FPA2015-65929-P and FIS2015-63770-P. C.G., M.C., and X.V. were partially supported by Grant FIS2014-54672-P from MINECO and FEDER, Grant 2014SGR-401 from Generalitat de Catalunya, and Project MDM-2014-0369 of ICCUB (Unidad de Excelencia María de Maeztu) from MINECO. C.G. also acknowledges Grant BES-2015-074210 from MINECO.

References

- [1] S.L. Shapiro, S.A. Teukolsky, *Black Holes, White Dwarfs, and Neutron Stars: The Physics of Compact Objects*, John Wiley & Sons, 1983.
- [2] P. Haensel, A.Y. Potekhin, D.G. Yakovlev, *Neutron Stars 1: Equation of State and Structure*, Springer, 2007.
- [3] G. Baym, C. Pethick, P. Sutherland, *Astrophys. J.* 170 (1971) 299.
- [4] J. Negele, D. Vautherin, *Nucl. Phys. A* 207 (1973) 298.
- [5] F. Douchin, P. Haensel, *Astron. Astrophys.* 380 (2001) 151.
- [6] B.K. Sharma, M. Centelles, X. Viñas, M. Baldo, G.F. Burgio, *Astron. Astrophys.* 584 (2015) A103.
- [7] M. Oertel, M. Hempel, T. Klähn, S. Typel, *Rev. Mod. Phys.* 89 (2017) 015007.
- [8] S. Goriely, N. Chamel, J.M. Pearson, *Phys. Rev. C* 82 (2010) 035804.
- [9] N. Chamel, A.F. Fantina, J.M. Pearson, S. Goriely, *Phys. Rev. C* 84 (2011) 062802.
- [10] A.F. Fantina, N. Chamel, J.M. Pearson, S. Goriely, *Astron. Astrophys.* 559 (2013) A128.
- [11] L. Guo, M. Hempel, J. Schaffner-Bielich, J.A. Maruhn, *Phys. Rev. C* 76 (2007) 065801.
- [12] H.S. Than, E. Khan, N.V. Giai, *J. Phys. G, Nucl. Part. Phys.* 38 (2011) 025201.
- [13] D.T. Loan, N.H. Tan, D.T. Khoa, J. Margueron, *Phys. Rev. C* 83 (2011) 065809.
- [14] J.M. Pearson, S. Goriely, N. Chamel, *Phys. Rev. C* 83 (2011) 065810.
- [15] R. Sellaheewa, A. Rios, *Phys. Rev. C* 90 (2014) 054327.
- [16] C. Gonzalez-Boquera, M. Centelles, X. Viñas, A. Rios, *Phys. Rev. C* 96 (2017) 065806.
- [17] J.M. Lattimer, F.D. Swesty, *Nucl. Phys. A* 535 (1991) 331.
- [18] H. Shen, H. Toki, K. Oyamatsu, K. Sumiyoshi, *Nucl. Phys. A* 637 (1998) 435.
- [19] J. Dechargé, D. Gogny, *Phys. Rev. C* 21 (1980) 1568.
- [20] J.F. Berger, M. Girod, D. Gogny, *Comput. Phys. Commun.* 63 (1991) 365.
- [21] F. Chappert, M. Girod, S. Hilaire, *Phys. Lett. B* 668 (2008) 420.
- [22] S. Goriely, S. Hilaire, M. Girod, S. Péru, *Phys. Rev. Lett.* 102 (2009) 242501.
- [23] G. Audi, M. Wang, A. Wapstra, F. Kondev, M. MacCormick, X. Xu, B. Pfeiffer, *Chin. Phys. C* 36 (2012) 1287.
- [24] B. Friedman, V. Pandharipande, *Nucl. Phys. A* 361 (1981) 502.
- [25] P.B. Demorest, T. Pennucci, S.M. Ransom, M.S.E. Roberts, J.W.T. Hessels, *Nature* 467 (2010) 1081.
- [26] J. Antoniadis, et al., *Science* 340 (2013) 448.
- [27] B.-A. Li, A. Ramos, G. Verde, I. Vidana, *Eur. Phys. J. A* 50 (2014) 9.
- [28] P. Danielewicz, J. Lee, *Nucl. Phys. A* 922 (2014) 1.
- [29] Z. Zhang, L.-W. Chen, *Phys. Rev. C* 92 (3) (2015) 031301.
- [30] M.B. Tsang, Y. Zhang, P. Danielewicz, M. Famiano, Z. Li, W.G. Lynch, A.W. Steiner, *Phys. Rev. Lett.* 102 (2009) 122701.
- [31] P. Danielewicz, R. Lacey, W.G. Lynch, *Science* 298 (2002) 1592.
- [32] F. Chappert, N. Pillet, M. Girod, J.-F. Berger, *Phys. Rev. C* 91 (2015) 034312.
- [33] F. Chappert, Ph.D. thesis, Université Paris-Sud XI, 2007, <https://tel.archives-ouvertes.fr/tel-00177379/en/>.
- [34] B. Link, R.I. Epstein, J.M. Lattimer, *Phys. Rev. Lett.* 83 (1999) 3362.
- [35] J. Carriere, C.J. Horowitz, J. Piekarewicz, *Astrophys. J.* 593 (2003) 463.
- [36] J. Xu, L.-W. Chen, B.-A. Li, H.-R. Ma, *Astrophys. J.* 697 (2009) 1549.
- [37] K. Hebeler, J.M. Lattimer, C.J. Pethick, A. Schwenk, *Astrophys. J.* 773 (1) (2013) 11.
- [38] J. Nättälä, A.W. Steiner, J.J.E. Kajava, V.F. Suleimanov, J. Poutanen, *Astron. Astrophys.* 591 (2016) A25.
- [39] J.M. Lattimer, A.W. Steiner, *Eur. Phys. J. A* 50 (2014) 40.
- [40] J.M. Lattimer, B.F. Schutz, *Astrophys. J.* 629 (2005) 979.
- [41] J.B. Hartle, *Astrophys. J.* 150 (1967) 1005.
- [42] A.G. Lyne, et al., *Science* 303 (2004) 1153.
- [43] N. Andersson, K. Glampedakis, W.C.G. Ho, C.M. Espinoza, *Phys. Rev. Lett.* 109 (2012) 241103.
- [44] N. Chamel, *Phys. Rev. Lett.* 110 (2013) 011101.
- [45] J. Piekarewicz, F.J. Fattoyev, C.J. Horowitz, *Phys. Rev. C* 90 (2014) 015803.
- [46] A.W. Steiner, S. Gandolfi, F.J. Fattoyev, W.G. Newton, *Phys. Rev. C* 91 (2015) 015804.
- [47] W.G. Newton, S. Berger, B. Haskell, *Mon. Not. R. Astron. Soc.* 454 (2015) 4400.
- [48] T. Delsate, N. Chamel, N. Gürlebeck, A.F. Fantina, J.M. Pearson, C. Ducoin, *Phys. Rev. D* 94 (2016) 023008.
- [49] X. Roca-Maza, M. Brenna, B.K. Agrawal, P.F. Bortignon, G. Colò, L.-G. Cao, N. Paar, D. Vretenar, *Phys. Rev. C* 87 (2013) 034301.
- [50] B.K. Agrawal, S. Shlomo, V.K. Au, *Phys. Rev. C* 72 (2005) 014310.
- [51] J. Piekarewicz, *Phys. Rev. C* 83 (2011) 034319.
- [52] F.J. Fattoyev, J. Piekarewicz, *Phys. Rev. Lett.* 111 (2013) 162501.
- [53] C.J. Horowitz, J. Piekarewicz, *Phys. Rev. Lett.* 86 (2001) 5647.
- [54] M. Centelles, X. Roca-Maza, X. Viñas, M. Warda, *Phys. Rev. Lett.* 102 (2009) 122502.
- [55] B.-A. Li, X. Han, *Phys. Lett. B* 727 (2013) 276.
- [56] J.M. Lattimer, Y. Lim, *Astrophys. J.* 771 (2013) 51.
- [57] X. Roca-Maza, X. Viñas, M. Centelles, B.K. Agrawal, G. Colo', N. Paar, J. Piekarewicz, D. Vretenar, *Phys. Rev. C* 92 (2015) 064304.
- [58] G. Hagen, et al., *Nat. Phys.* 12 (2015) 186.
- [59] J. Birkhan, et al., *Phys. Rev. Lett.* 118 (2017) 252501.
- [60] W.-C. Chen, J. Piekarewicz, *Phys. Lett. B* 748 (2015) 284.
- [61] L. Tolos, M. Centelles, A. Ramos, *Astrophys. J.* 834 (2017) 3.
- [62] L.M. Robledo, *HFBaxial computer code*, 2002.
- [63] L.M. Robledo, G.F. Bertsch, *Phys. Rev. C* 84 (2011) 014312.
- [64] L.M. Robledo, G.F. Bertsch, *Phys. Rev. C* 84 (2011) 054302.
- [65] R.R. Rodríguez-Guzmán, J.L. Egido, L.M. Robledo, *Phys. Rev. C* 62 (2000) 054319.
- [66] S. Hilaire, M. Girod, *Eur. Phys. J. A* 33 (2007) 237.
- [67] M. Baldo, L.M. Robledo, P. Schuck, X. Viñas, *Phys. Rev. C* 87 (2013) 064305.
- [68] L.M. Robledo, *J. Phys. G, Nucl. Part. Phys.* 42 (5) (2015) 055109.
- [69] N. Pillet, S. Hilaire, *Eur. Phys. J. A* 53 (2017) 193.
- [70] B. Alex Brown, *Phys. Rev. Lett.* 85 (2000) 5296.